

Original Article

Application of quantitative orbital analysis to assess the activity of Graves' ophthalmopathy

Shuang Li¹, Yue-Jun Liu²

¹Department of Nuclear Medicine, Xiangyang No. 1 People's Hospital, Hubei University of Medicine, Xiangyang 441000, Hubei, China; ²Department of Ophthalmology, Xiangyang No. 1 People's Hospital, Hubei University of Medicine, Xiangyang 441000, Hubei, China

Received August 18, 2023; Accepted October 16, 2023; Epub December 25, 2023; Published December 30, 2023

Abstract: This study aimed to evaluate the diagnostic value of uptake ratios in the extraocular muscles (EOMs), lacrimal glands, and optic nerves to detect the inflammation activity of Graves' ophthalmopathy (GO) using quantitative analysis of 99m technetium (^{99m}Tc)-labeled diethylene triamine pentaacetic acid (DTPA) orbital single-photon emission computed tomography/computed tomography (SPECT/CT) images. The patients were categorized into an active stage (clinical activity score $\geq 3/7$, n=23) or an inactive stage (clinical activity score $< 3/7$, n=38), based on their clinical activity score. The uptake ratio was manually determined by placing a region of interest within the area of highest uptake, as agreed upon by consensus, in the EOMs, lacrimal gland, and optic nerve on SPECT images corrected for CT attenuation. Patients with active GO exhibited significantly higher uptake ratios in the EOMs, lacrimal glands, and optic nerves compared to patients with inactive GO (all $P < 0.01$). These parameters have been proven effective in differentiating between active and inactive disease.

Keywords: Graves' ophthalmopathy, ^{99m}Tc-DTPA, uptake ratio, extraocular muscle, lacrimal gland, optic nerve

Introduction

Graves' ophthalmopathy (GO) is characterized by autoimmune inflammation affecting the extraocular muscles (EOMs) and connective tissue surrounding the orbit, usually in patients with Graves' disease [1, 2]. A prominent feature of GO is exophthalmos, which is caused by the enlargement of EOMs [3]. Other typical symptoms of GO include bulging eyes, swelling around orbital tissues, and retracted eyelids. Patients may also experience ocular motility disorders and diplopia owing to the involvement of EOMs. In severe cases, visual impairments such as vision loss, compressed optic neuropathy, reduced visual acuity, and even blindness may occur [4]. Studies have shown that pharmacological interventions in patients with GO in the early inflammatory phase can reduce the clinical activity and severity of GO. However, as the disease progresses to a certain level, conventional medical treatments become ineffective and orbital decompression is required. Therefore, an accurate disease

assessment is essential for the diagnosis and treatment of GO [5].

Clinicians primarily rely on the clinical activity score (CAS) to guide the treatment of patients with GO. However, CAS may not adequately evaluate the acute inflammatory impairment of EOMs or orbital fat, especially in the absence of diplopia or motility disorders. Combining imaging indices with CAS can improve the sensitivity of detection of inflammatory activity and the prediction of treatment response. Orbital single-photon emission computed tomography/computed tomography (SPECT/CT) octreotide imaging is considered the most accurate method for evaluating periorbital inflammation in GO. However, it is not widely available in China because of the cost and imaging time constraints [6-8]. An alternative diagnostic method is the use of 99m technetium (^{99m}Tc)-labeled diethylene triamine pentaacetic acid (DTPA), a sensitive indicator of inflammatory activity. Compared with octreotide imaging, ^{99m}Tc-DTPA imaging is more economical, easier to label,

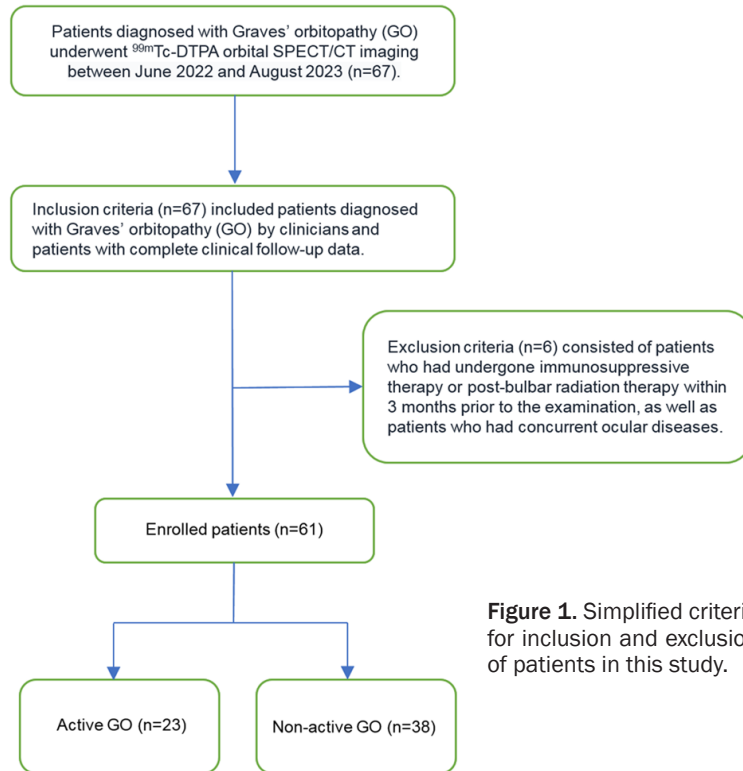


Figure 1. Simplified criteria for inclusion and exclusion of patients in this study.

Materials and methods

Case date

In this retrospective analysis, 67 patients diagnosed with GO underwent ^{99m}Tc-DTPA orbital SPECT/CT scanning at Xiangyang No. 1 People’s Hospital between July 2022 and June 2023. The collected clinical data included age, sex, smoking status, CAS, and history of immunosuppressive therapy or other eye diseases. The inclusion criteria were patients with GO diagnosed by clinicians, patients with complete clinical follow-up data. The exclusion criteria were patients who had undergone immunosuppressive therapy or post-bulbar radiation therapy within three months preceding the examination, and patients with other ocular diseases. Based on the exclusion cri-

and has a shorter imaging time. Several studies have reported good agreement between ^{99m}Tc-DTPA orbital SPECT/CT and both CAS and octreotide imaging for assessing the degree of orbital inflammation [9, 10]. This process-specific image has been shown to directly indicate the inflammatory activity of the orbit affected by GO [11].

Active GO is characterized by inflammatory infiltration of the EOMs, lacrimal gland, and optic nerve, often involving both eyes [12]. Therefore, this study aimed to evaluate the inflammatory activity of GO by analyzing the SPECT/CT parameters of EOMs, lacrimal glands, and optic nerves. The quantitative analysis technique used in this study can directly display the inflammatory reaction of the EOM, lacrimal gland, and optic nerve, enabling accurate localization of the involved structures. Additionally, SPECT/CT can measure the uptake ratio (UR) value of each EOM, lacrimal gland, and optic nerve, providing a more accurate evaluation of the degree of inflammatory activity in GO. These findings serve as an essential reference for the clinical diagnosis and treatment of GO.

teria, six patients were excluded, resulting in the final enrollment of 61 patients with GO. All patients were classified into either the active stage (CAS ≥ 3/7, n=23) or the inactive stage (CAS < 3/7, n=38) according to their CAS (**Figure 1**). Assessment of each patient’s condition and their CAS calculation was performed by an endocrinologist ranked as an attending physician or higher, whereas the assessment of their eye status was conducted by an ophthalmologist ranked as an attending physician or higher.

This study was approved by the Institutional Review Board of Xiangyang No. 1 Hospital (Issue No. 2021KYLX) and conducted in accordance with the principles of the Declaration of Helsinki. Written informed consent was obtained from all patients who underwent SPECT/CT examinations.

SPECT/CT scanning

Orbital SPECT/CT imaging was performed using an NM 860 system (General Electric Company, USA) with low power consumption and a high-resolution parallel-bore collimator. Prior to or-

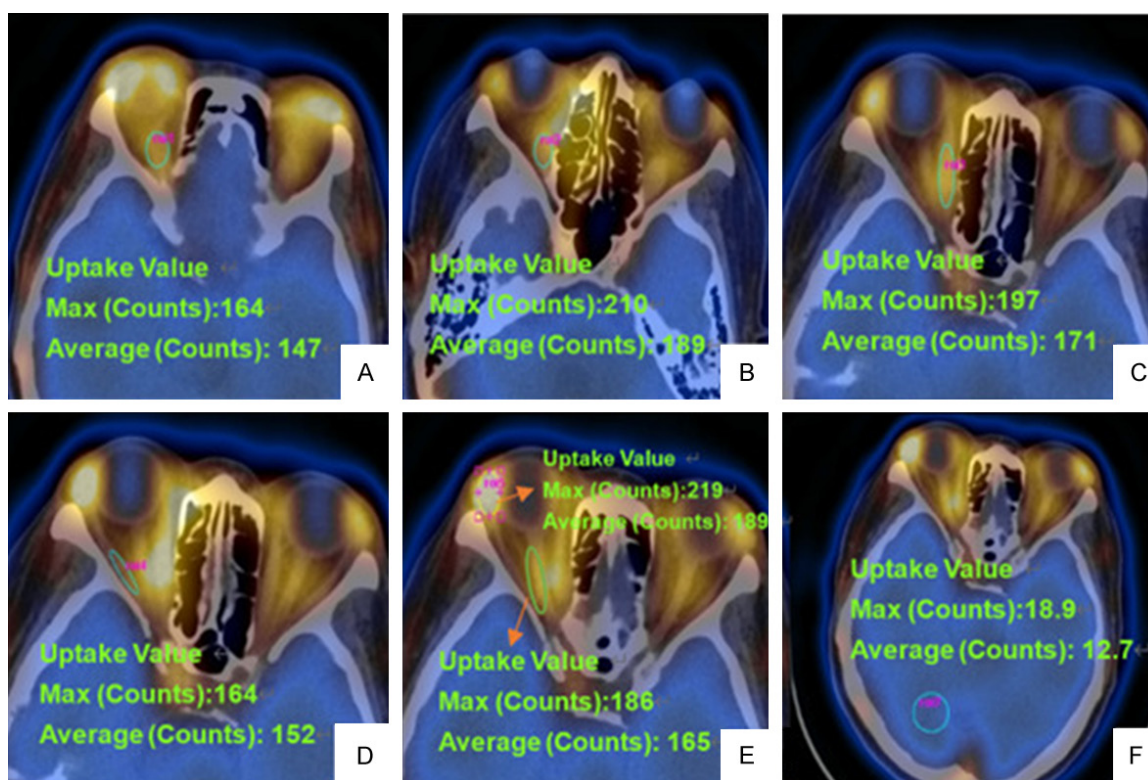


Figure 2. The schematic diagram used to measure the ROI parameters of ^{99m}Tc -DTPA orbital SPECT/CT images of GO. The uptake values were manually determined by placing a ROI within the area showing the highest uptake in the EOM, lacrimal gland, and optic nerve, according to the consensus on SPECT images corrected for CT attenuation. A. Super rectus uptake value. B. Inferior rectus uptake value. C. Medial rectus uptake value. D. Lateral rectus uptake value. E. Lacrimal gland and optic nerve uptake value. F. To determine the background uptake value, a circular ROI was placed on the occipital lobe at the optic nerve level. The uptake values of the EOM, lacrimal gland, and optic nerve relative to the background uptake values were then calculated. ROI, region of interest.

bital SPECT/CT scanning, an intravenous infusion of 555 MBq ^{99m}Tc -DTPA (China Institute of Atomic Energy, Beijing, China, with a radiochemical purity of over 95%) was administered over a period of 20 min. SPECT scanning was conducted using Zoom 1.33 and a matrix size of 64×64 , a peak of 140 keV, and a window width of 20%. The CT scanning parameters were as follows: tube voltage, 140 kV; tube current, 100 mA; and slice thickness, 1 mm. The fusion of SPECT and CT images was achieved through co-located fusion using GE Xeleris 3.0 workstation image processing software.

The uptake values were manually determined by placing a region of interest (ROI) within the area showing the highest uptake in the EOM, lacrimal gland, and optic nerve, according to the consensus on SPECT images corrected for CT attenuation. To determine the background uptake value, a circular ROI was placed on the occipital lobe at the optic nerve level. In a previ-

ous study, the UR value was calculated as the ratio of the maximum uptake value in the ROI to the maximum uptake value in the background [10]. The uptake values of the EOM, lacrimal gland, and optic nerve relative to the background uptake values were then calculated. Furthermore, the maximum UR among the four EOMs was selected as URmax. The SPECT/CT ROI parameters were measured according to the method shown in **Figure 2**.

Statistical methods

The statistical analysis was conducted with the help of the SPSS 25.0 software. The measurements are expressed as mean \pm standard deviation ($\bar{x} \pm s$). Based on the nature of the data, comparisons between continuous variable groups were conducted using the t-test or U-test. Spearman's rank correlation analysis was used to examine the correlation between UR and CAS. Receiver operating characteristic

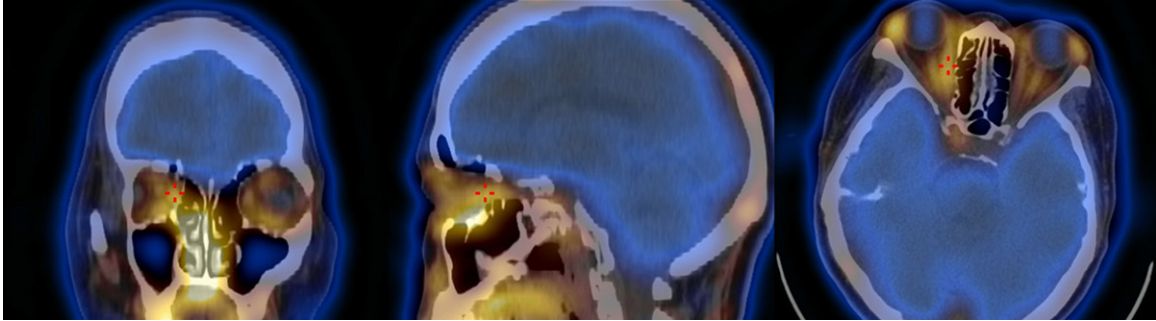


Figure 3. The images presented from left to right depict the coronal image, sagittal image, and transverse image of the orbital SPECT/CT. Patients with active GO showed significantly increased radionuclide uptake in orbital tissues such as EOMs, lacrimal glands, optic nerves, and posterior bulbar fat.



Figure 4. The images presented from left to right depict the coronal image, sagittal image, and transverse image of the orbital SPECT/CT. Patients with inactive GO showed mildly increased or unchanged radionuclide uptake in orbital tissues such as EOMs, lacrimal glands, optic nerves, and posterior bulbar fat.

(ROC) curve analysis was employed to evaluate the predictive models for diagnosing GO activity using the UR of the EOMs, lacrimal glands, optic nerves, and URmax. A significance level of $P < 0.05$ was considered statistically significant.

Results

The visual analysis of ^{99m}Tc -DTPA orbital SPECT/CT images

Based on the orbital SPECT/CT images of all patients, patients with active GO showed significantly increased radionuclide uptake in orbital tissues, such as EOMs, lacrimal glands, optic nerves, and posterior bulbar fat (**Figure 3**). In contrast, patients with inactive GO exhibited mildly increased or unchanged radionuclide uptake (**Figure 4**).

Results of ^{99m}Tc -DTPA orbital SPECT/CT quantitative analysis

According to the CAS, all patients were divided into an active group ($\text{CAS} \geq 3/7$, $n=23$) and an

inactive group ($\text{CAS} < 3/7$, $n=38$). The average age of the active GO group was 43 ± 11 years, and the average age of the inactive GO group was 38 ± 12 years. In the active GO group, 52.2% (12 of 23) were female, whereas in the inactive GO group, 55.3% (21 of 38) were female. The proportion of patients with a history of smoking was 34.8% (8 patients) in the active GO group and 21.1% (8 patients) in the inactive GO group. There were no significant differences between the two groups in terms of sex, age, or smoking history ($P=0.814$, 0.718 , and 0.368 , respectively). The patients with active GO exhibited a significantly higher UR for the EOMs, lacrimal gland, and optic nerve than patients with inactive GO (all $P < 0.01$) (**Table 1**; **Figure 5**). These results indicate that using these parameters can effectively differentiate between active and inactive GO.

Correlation analysis of UR and CAS

Spearman's rank correlation analysis was conducted to investigate the relationship between the UR of the EOMs, the lacrimal gland, the

Table 1. Comparison of uptake ratio between active and inactive GO patients

	Active GO	Inactive GO	P
Female, n (%)	12 (52.2)	21 (55.3)	.814
Age (years)	43±11	38±12	.718
Smokers, n (%)	8 (34.8)	8 (21.1)	.368
CAS, points	3.78±1.1	1.61±0.49	.000
Uptake ratio (UR), no unit			
SR	4.91±1.63	4.02±1.15	.001
IR	5.27±1.49	4.25±1.06	.000
MR	5.56±1.70	4.36±1.17	.000
LR	4.98±1.31	4.21±1.07	.001
URmax	6.18±1.95	4.85±1.11	.003
LG	6.14±1.84	5.41±1.00	.005
ON	5.12±1.39	4.41±1.03	.001

LR, lateral rectus; MR, medial rectus; SR, super rectus; IR, inferior rectus; URmax, maximum uptake ratio among the four EOMs; LG, lacrimal gland; ON, optic nerve; CAS, clinical activity score. There were no significant differences between the two groups in terms of sex, age, or smoking history ($P=0.814$, 0.718 , and 0.368 , respectively). The patients with active GO exhibited a significantly higher UR for the EOMs, lacrimal gland, and optic nerve than patients with inactive GO (all $P < 0.01$). These results indicate that using these parameters can effectively differentiate between active and inactive GO.

optic nerve, and the URmax with CAS. The results indicated that there was a correlation between the UR of the EOMs, the lacrimal gland, the optic nerve, and URmax with CAS ($r=0.517$, 0.497 , 0.388 , and 0.624 , respectively, $P < 0.01$). This indicates that the UR of the EOMs, lacrimal gland, optic nerve, and URmax exhibited a positive response in terms of inflammatory activity. Considering URmax as the most severely affected EOM imaging indicator, it is evident that URmax has a strong correlation with CAS (Table 2).

ROC curve analysis of UR

ROC curve analysis was conducted to assess the predictive performance of the UR models. The URmax model demonstrated the highest reliable prognostic performance, with an area under the curve (AUC) of 0.803, (95% confidence interval [CI] [0.763-0.842]). The EOMs, lacrimal gland, and optic nerve models also showed comparatively better predictive performance (0.730, [0.686-0.775], 0.786, [0.746-0.827], and 0.635, [0.586-0.684], respectively; $P < 0.01$). This result confirmed that the URmax model exhibited the most effective predictive performance (Table 3; Figure 6).

Discussion

The etiology of GO is not fully understood, but current research suggests that it has a multifactorial etiology involving both cellular and humoral immune responses as well as genetic and environmental influences. During the inactive phase of GO, histological changes primarily involve fibrosis of the EOMs and hyperplasia of the posterior bulb fat. Conversely, during the active phase, there is significant lymphocyte infiltration and subsequent cytokine release, which leads to fibroblast activation and hyaluronic acid accumulation, among other processes [13-15].

Imaging indices combined with CAS have shown improved sensitivity for detecting inflammatory activity and predicting treatment responses. Various imaging techniques, such as ultrasound, orbital CT, ma-

netic resonance imaging (MRI), and nuclear medicine, have been gradually applied for the clinical diagnosis of GO patients [16]. Among the imaging methods used to aid in the diagnosis of GO, ultrasound is the preferred choice in clinical practice. It can be used to assess the degree of enlargement and inflammatory infiltration in EOMs. However, its disadvantages include poor visualization of the orbital apex region, inaccurate measurements, and subjective variations in results [17]. CT uses X-rays to diagnose and differentiate diseases based on different absorption levels in various tissues. It can quantify the degree of enlargement of EOMs and diagnose GO by analyzing tissues such as EOMs, orbital fat, and lacrimal glands [18]. Although CT has a lower sensitivity in determining the activity of GO than ultrasound and MRI, it has significant advantages in evaluating the efficacy of decompression surgery in patients with late-stage GO and selecting the optimal surgical approach. MRI has a high soft-tissue resolution, which provides a unique advantage in assessing the inflammation of the orbital tissues in GO. It can also be used to monitor the effectiveness of clinical treatments. T2-weighted imaging (T2WI) can accurately depict EOM edema, inflammatory infiltra-

Uptake ratio between active and inactive GO patients

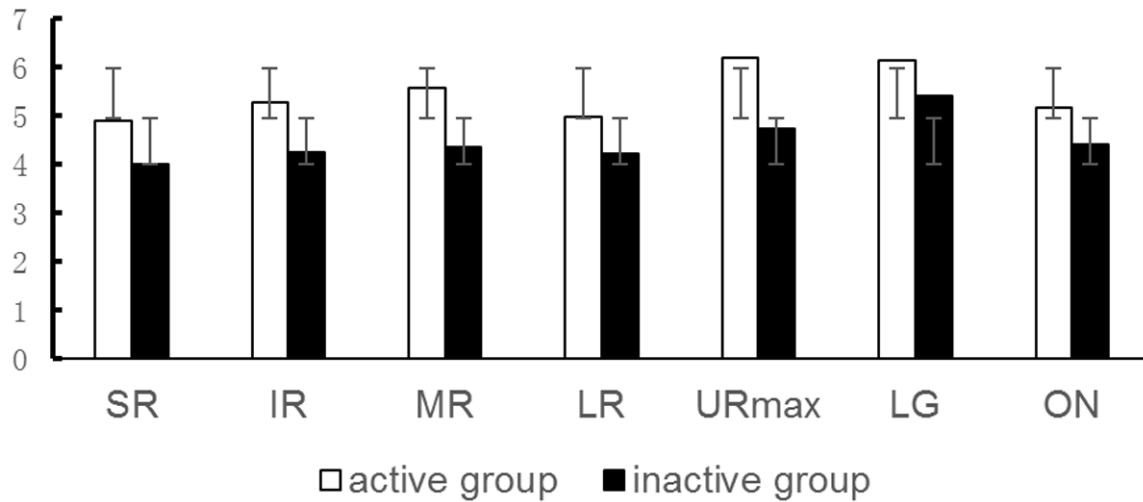


Figure 5. The patients with active Graves’ orbitopathy exhibited a significantly higher uptake ratio of each extraocular muscle, lacrimal gland, optic nerve and URmax in comparison to those patients with inactive GO.

Table 2. A Spearman’s rank correlation analysis was performed to investigate the relationship between the UR of EOMS, lacrimal gland, optic nerve and URmax with the CAS

	r	P
EOMS	0.517	.000
URmax	0.624	.000
LG	0.497	.000
ON	0.388	.000

The results indicated that there was a correlation between the UR of the EOMS, the lacrimal gland, the optic nerve, and URmax with CAS ($r=0.517, 0.497, 0.388,$ and $0.624,$ respectively, $P < 0.01$). This indicates that the UR of the EOMS, lacrimal gland, optic nerve, and URmax exhibited a positive response in terms of inflammatory activity. Considering URmax as the most severely affected EOM imaging indicator, it is evident that URmax has a strong correlation with CAS. EOMS, extraocular muscles; URmax, maximum uptake ratio among the four EOMS; LG, lacrimal gland; ON, optic nerve; CAS, Clinical Activity Score.

Table 3. ROC curve analysis was conducted to assess the predictive performance of the UR EOMS, lacrimal gland, optic nerve and URmax

	Area	Asymptotic 95% Confidence Interval	P
EOMS	.730	(.686, .775)	.000
URmax	.803	(.690, .915)	.000
LG	.786	(.706, .867)	.000
ON	.635	(.537, .733)	.000

The URmax model demonstrated the highest reliable prognostic performance, with an area under the curve (AUC) of 0.803, (95% confidence interval [CI] [0.763-0.842]). The EOMS, lacrimal gland, and optic nerve models also showed comparatively better predictive performance (0.730, [0.686-0.775], 0.786, [0.746-0.827], and 0.635, [0.586-0.684], respectively; $P < 0.01$). This result confirmed that the URmax model exhibited the most effective predictive performance. EOMS, extraocular muscles; URmax, maximum uptake ratio among the four EOMS; LG, lacrimal gland; ON, optic nerve.

tion, and fibrosis, assisting in determining disease activity status. This is of significant value for staging GO activity [19-24].

Nuclear medicine ^{99m}Tc -DTPA orbital SPECT/CT produces homogeneous tomographic images that provide both functional information of the orbit through SPECT and anatomical information of the orbit through CT localization and di-

agnosis; these images allow the target tissue to be accurately outlined for the development of quantitative parameters. As the study of ^{99m}Tc -DTPA orbital SPECT/CT imaging advances, there is an increasing need for objective quantitative indicators to fine-tune disease assessment and efficacy. ^{99m}Tc -DTPA orbital SPECT/CT imaging provides both visual and semi-quantitative data on GO orbital inflammatory activity.

Molecular imaging of GO

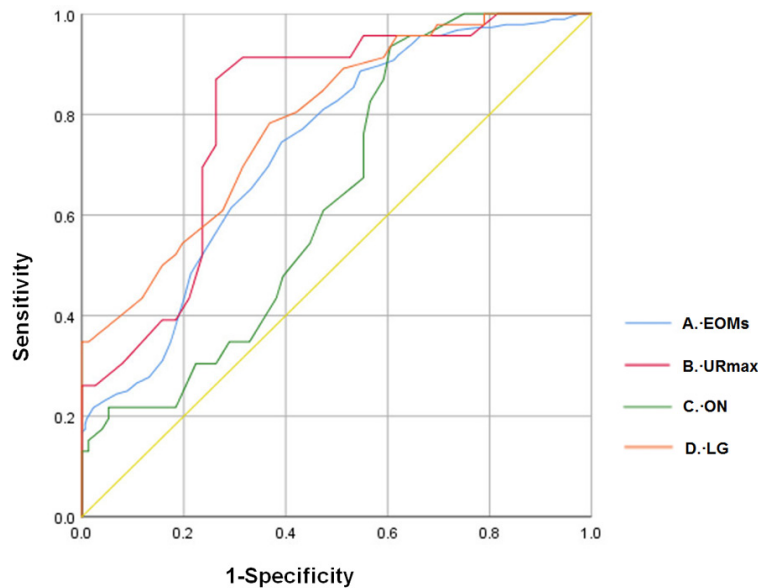


Figure 6. ROC curve analysis was conducted to assess the predictive performance of the UR models. A. EOMs model; B. URmax model; C. Optic nerve model; D. Lacrimal gland model; ROC, Receiver operating characteristic; AUC, area under the curve. Among the models, the URmax model exhibited the highest reliability in terms of prognostic performance.

Previous studies [25-28] used ^{99m}Tc -DTPA orbital SPECT to assess autoimmune inflammation in the orbital regions of patients with GO. However, these scans only allow analysis of the retrobulbar or overall orbital areas, without providing detailed information on the specific affected orbital tissues. With advances in ^{99m}Tc -DTPA orbital SPECT/CT imaging, there is an increasing need for objective quantitative indicators to enhance disease assessment and efficacy.

Compared with the retrobulbar or overall orbital UR values for the assessment of the inflammatory activity of GO, the EOM assessment had higher sensitivity and better objectivity. Murakami et al. [29] reported that patients with GO often presented with one or more EOMs. In their study of 184 patients with EOM enlargement, they found that 54% of patients had hypertrophy of a single muscle, 25% had hypertrophy of two muscles, 12% had hypertrophy of three muscles, and 9% had hypertrophy of all four muscles. Considering that different stages of the disease may exist in each EOM, we conducted the UR of each EOM separately in this study. A correlation analysis was conducted to examine the relationship between the UR of the four EOMs and URmax with CAS to evaluate the

diagnostic efficacy of the inflammatory activity of GO. We found that URmax achieved the best results in the activity assessment, suggesting that the URmax (the most severely affected EOM) had the strongest association with the disease. An increase in UR of a particular EOM in the orbit may indicate disease activity.

GO progression is accompanied by changes in the lacrimal gland, including protruding eyes, upper eyelid recession, and widening of lid fissures. These changes result in uneven distribution of tears on the ocular surface, shortened tear film rupture time, accelerated tear evaporation, and increased osmotic pressure. Consequently, these factors contribute to a decrease in the

secretory function [30-32]. The pathophysiological changes in lacrimal gland involvement are similar to those in retrobulbar tissue involvement, both showing multifocal infiltration of lymphocytes and adipose tissue hyperplasia [33]. Subsequently, we conducted a comprehensive analysis of nuclear imaging findings in the lacrimal gland. We observed that the nuclide concentration was generally consistent with the uptake of nuclides by the EOMs. Furthermore, the UR of the lacrimal gland was significantly higher in the active group than in the inactive group. Zhao et al. [34, 35] retrospectively analyzed 81 patients with GO and found that patients with active GO had higher UR of the lacrimal gland than those with inactive GO.

Dysthyroid optic neuropathy is a severe complication of GO caused by dysfunction of the optic nerve and may result in permanent visual loss [36, 37]. The pathogenesis of dysthyroid optic neuropathy is generally considered to be primarily due to optic nerve compression and ischemic changes caused by tissue congestion at the orbital apex, high orbital pressure, and optic nerve entrapment [24, 38]. Thus, our study found that patients with active GO exhibited significantly higher UR of the optic nerve

than patients with inactive GO. Therefore, we suggest that optic nerve lesions may be related to extensive optic nerve damage caused by inflammation of the optic nerve and loss of myelin sheaths and axons.

By utilizing orbital SPECT/CT imaging, this study demonstrated increased radionuclide uptake in the orbital tissues of patients with active GO compared to those with inactive GO. The UR of the EOMs, lacrimal glands, optic nerves and URmax were significantly higher in patients with active GO, and these parameters were significantly correlated with CAS. ROC curve analysis further confirmed the predictive efficacy of the UR models, with the URmax model exhibiting the best performance. Based on quantitative orbital analysis, clinicians may be able to assess the inflammatory activity of GO more precisely.

This study has certain limitations. 1) The study cohort did not have a homogeneous distribution of patients with moderate-to-severe GO, with a higher proportion having a CAS of 3 or 4 and fewer having a CAS of 6 or 7. This can lead to a reduced accuracy of the results. Mild GO has a minimal impact on daily life, whereas moderate-to-severe GO has the potential to induce corneal and optic nerve damage, even leading to blindness. 2) It should be noted that this study was cross-sectional and lacked a longitudinal design and a large sample size. The early stages of GO are characterized by edema and inflammatory cell infiltration in the EOMs and orbital connective tissue, whereas advanced stages of the disease may lead to keratitis, dry eye, and optic nerve compression. Future longitudinal experiments with larger sample sizes will provide further clarification.

Further research and validation of these findings are warranted to establish orbital SPECT/CT as a valuable tool for the clinical management of patients with GO.

Disclosure of conflict of interest

None.

Address correspondence to: Yue-Jun Liu, Department of Ophthalmology, Xiangyang No. 1 People's Hospital, Hubei University of Medicine, Xiangyang 441000, Hubei, China. Tel: +86-13871668700; E-mail: 49275810@qq.com

References

- [1] Wiersinga WM. Advances in treatment of active, moderate-to-severe Graves' ophthalmopathy. *Lancet Diabetes Endocrinol* 2017; 5: 134-142.
- [2] Yao N, Li L, Gao Z, Zhao C, Li Y, Han C, Nan J, Zhu Z, Xiao Y, Zhu F, Zhao M and Zhou W. Deep learning-based diagnosis of disease activity in patients with Graves' orbitopathy using orbital SPECT/CT. *Eur J Nucl Med Mol Imaging* 2023; 50: 3666-3674.
- [3] Bartalena L and Tanda ML. Current concepts regarding Graves' orbitopathy. *J Intern Med* 2022; 292: 692-716.
- [4] Bartalena L, Kahaly GJ, Baldeschi L, Dayan CM, Eckstein A, Marcocci C, Marinò M, Vaidya B and Wiersinga WM; EUGOGO†. The 2021 European Group on Graves' orbitopathy (EUGOGO) clinical practice guidelines for the medical management of Graves' orbitopathy. *Eur J Endocrinol* 2021; 185: G43-G67.
- [5] Taylor PN, Zhang L, Lee RWJ, Muller I, Ezra DG, Dayan CM, Kahaly GJ and Ludgate M. New insights into the pathogenesis and nonsurgical management of Graves orbitopathy. *Nat Rev Endocrinol* 2020; 16: 104-116.
- [6] Sun B, Zhang Z, Dong C, Zhang Y, Yan C and Li S; Medscape. (99)Tc(m)-octreotide scintigraphy and serum eye muscle antibodies in evaluation of active thyroid-associated ophthalmopathy. *Eye (Lond)* 2017; 31: 668-676.
- [7] Kim SE, Kim J, Lee JY, Lee SB, Paik JS and Yang SW. Octreotide inhibits secretion of IGF-1 from orbital fibroblasts in patients with thyroid-associated ophthalmopathy via inhibition of the NF-κB pathway. *PLoS One* 2021; 16: e0249988.
- [8] Gomes-Porras M, Cárdenas-Salas J and Álvarez-Escolá C. Somatostatin analogs in clinical practice: a review. *Int J Mol Sci* 2020; 21: 1682.
- [9] Galuska L, Leovey A, Szucs-Farkas Z, Szabados L, Garai I, Berta A, Balazs E, Varga J and Nagy EV. Imaging of disease activity in Graves' orbitopathy with different methods: comparison of (99m)Tc-DTPA and (99m)Tc-depreotide single photon emission tomography, magnetic resonance imaging and clinical activity scores. *Nucl Med Commun* 2005; 26: 407-414.
- [10] Jiang C, Deng Z, Huang J, Deng H, Tan J, Li X and Zhao M. Monitoring and predicting treatment response of extraocular muscles in Grave's orbitopathy by (99m)Tc-DTPA SPECT/CT. *Front Med (Lausanne)* 2021; 8: 791131.
- [11] Szumowski P, Abdelrazek S, Żukowski Ł, Mojsak M, Sykała M, Siewko K, Maliszewska K, Popławska-Kita A and Myśliwiec J. Efficacy of (99m)Tc-DTPA SPECT/CT in diagnosing orbi-

- topathy in Graves' disease. *BMC Endocr Disord* 2019; 19: 10.
- [12] Bartalena L, Piantanida E, Gallo D, Lai A and Tanda ML. Epidemiology, natural history, risk factors, and prevention of Graves' orbitopathy. *Front Endocrinol (Lausanne)* 2020; 11: 615993.
- [13] Virakul S, Heutz JW, Dalm VA, Peeters RP, Paridaens D, van den Bosch WA, Hirankarn N, van Hagen PM and Dik WA. Basic FGF and PDGF-BB synergistically stimulate hyaluronan and IL-6 production by orbital fibroblasts. *Mol Cell Endocrinol* 2016; 433: 94-104.
- [14] Yu CY, Ford RL, Wester ST and Shriver EM. Update on thyroid eye disease: regional variations in prevalence, diagnosis, and management. *Indian J Ophthalmol* 2022; 70: 2335-2345.
- [15] Lehmann GM, Feldon SE, Smith TJ and Phipps RP. Immune mechanisms in thyroid eye disease. *Thyroid* 2008; 18: 959-965.
- [16] Kahaly GJ. Recent developments in Graves' ophthalmopathy imaging. *J Endocrinol Invest* 2004; 27: 254-258.
- [17] Yuksel N, Unal O, Mutlu M, Ergeldi G and Caglayan M. Real-time ultrasound elastographic evaluation of extraocular muscle involvement in Graves' ophthalmopathy. *Orbit* 2020; 39: 160-164.
- [18] Lee SH, Lee S, Lee J, Lee JK and Moon NJ. Effective encoder-decoder neural network for segmentation of orbital tissue in computed tomography images of Graves' orbitopathy patients. *PLoS One* 2023; 18: e0285488.
- [19] Hu H, Chen L, Zhou J, Chen W, Chen HH, Zhang JL, Hsu YC, Xu XQ and Wu FY. Multiparametric magnetic resonance imaging for differentiating active from inactive thyroid-associated ophthalmopathy: added value from magnetization transfer imaging. *Eur J Radiol* 2022; 151: 110295.
- [20] Zhai L, Wang Q, Liu P, Luo B, Yuan G and Zhang J. T2 mapping with and without fat-suppression to predict treatment response to intravenous glucocorticoid therapy for thyroid-associated ophthalmopathy. *Korean J Radiol* 2022; 23: 664-673.
- [21] Li Z, Luo Y, Feng X, Zhang Q, Zhong Q, Weng C, Chen Z and Shen J. Application of multiparameter quantitative magnetic resonance imaging in the evaluation of Graves' ophthalmopathy. *J Magn Reson Imaging* 2023; 58: 1279-1289.
- [22] Keene KR, van Vught L, van de Velde NM, Ciggaar IA, Notting IC, Genders SW, Verschuuren JJGM, Tannemaat MR, Kan HE and Beenakker JM. The feasibility of quantitative MRI of extraocular muscles in myasthenia gravis and Graves' orbitopathy. *NMR Biomed* 2021; 34: e4407.
- [23] Čivrný J, Karhanová M, Hübnerová P, Schovánek J and Heřman M. MRI in the assessment of thyroid-associated orbitopathy activity. *Clin Radiol* 2022; 77: 925-934.
- [24] Chen HH, Hu H, Chen W, Cui D, Xu XQ, Wu FY and Yang T. Thyroid-associated orbitopathy: evaluating microstructural changes of extraocular muscles and optic nerves using readout-segmented echo-planar imaging-based diffusion tensor imaging. *Korean J Radiol* 2020; 21: 332-340.
- [25] Galuska L, Barna SK, Varga J, Garai I and Nagy EV. The role of 99mTc-DTPA retrobulbar SPECT in staging and follow-up of Graves' orbitopathy. *Nucl Med Rev Cent East Eur* 2018; 21: 54-58.
- [26] Ujhelyi B, Erdei A, Galuska L, Varga J, Szabados L, Balazs E, Bodor M, Cseke B, Karanyi Z, Leovey A, Mezosi E, Burman KD, Berta A and Nagy EV. Retrobulbar 99mTc-diethylenetriamine-pentaacetic-acid uptake may predict the effectiveness of immunosuppressive therapy in Graves' ophthalmopathy. *Thyroid* 2009; 19: 375-380.
- [27] Liu D, Xu X, Wang S, Jiang C, Li X, Tan J and Deng Z. 99mTc-DTPA SPECT/CT provided guide on triamcinolone therapy in Graves' ophthalmopathy patients. *Int Ophthalmol* 2020; 40: 553-561.
- [28] Zhong P, Yang J, Wang Y, Wei L and Chen L. Thyroid accumulation of 99mTc-DTPA in graves disease. *Clin Nucl Med* 2023; 48: e552-e553.
- [29] Murakami Y, Kanamoto T, Tuboi T, Maeda T and Inoue Y. Evaluation of extraocular muscle enlargement in dysthyroid ophthalmopathy. *Jpn J Ophthalmol* 2001; 45: 622-627.
- [30] Harris MA, Realini T, Hogg JP and Sivak-Callcott JA. CT dimensions of the lacrimal gland in graves orbitopathy. *Ophthalmic Plast Reconstr Surg* 2012; 28: 69-72.
- [31] Gao Y, Chang Q, Li Y, Zhang H, Hou Z, Zhang Z, Li Z and Li D. Correlation between extent of lacrimal gland prolapse and clinical features of thyroid-associated ophthalmopathy: a retrospective observational study. *BMC Ophthalmol* 2022; 22: 66.
- [32] Gounder P, Oliphant H, Juniat V, Koenig M, Selva D and Rajak SN. Histopathological features of asymmetric lacrimal gland enlargement in patients with thyroid eye disease. *Thyroid Res* 2023; 16: 32.
- [33] Huh HD, Kim JH, Kim SJ, Yoo JM and Seo SW. The change of lacrimal gland volume in Korean patients with thyroid-associated ophthalmopathy. *Korean J Ophthalmol* 2016; 30: 319-325.
- [34] Jiang C, Li X, Zhao M, Dend H, Huang J, Liu D and Xu X. Efficacy of 99mTc-DTPA orbital SPECT/CT on the evaluation of lacrimal gland inflammation in patients with thyroid associat-

Molecular imaging of GO

- ed ophthalmopathy. Zhong Nan Da Xue Xue Bao Yi Xue Ban 2019; 44: 322-328.
- [35] Zhao RX, Shi TT, Luo S, Liu YF, Xin Z and Yang JK. The value of SPECT/CT imaging of lacrimal glands as a means of assessing the activity of Graves' orbitopathy. Endocr Connect 2022; 11: e210590.
- [36] Dolman PJ. Dysthyroid optic neuropathy: evaluation and management. J Endocrinol Invest 2021; 44: 421-429.
- [37] Gonçalves AC, Gebrim EM and Monteiro ML. Imaging studies for diagnosing Graves' orbitopathy and dysthyroid optic neuropathy. Clinics (Sao Paulo) 2012; 67: 1327-1334.
- [38] Liu P, Luo B, Zhai LH, Wu HY, Wang QX, Yuan G, Jiang GH, Chen L and Zhang J. Multi-parametric diffusion tensor imaging of the optic nerve for detection of dysthyroid optic neuropathy in patients with thyroid-associated ophthalmopathy. Front Endocrinol (Lausanne) 2022; 13: 851143.